JPE 17-4-14

https://doi.org/10.6113/JPE.2017.17.4.983
ISSN(Print): 1598-2092 / ISSN(Online): 2093-4718

Performance Improvement of Model Predictive Control Using Control Error Compensation for Power Electronic Converters Based on the Lyapunov Function

Guiping Du†, Zhifei Liu*, Fada Du*, and Jiajian Li*

†,*School of Electric Power, South China University of Technology, Guangzhou, China

Abstract

This paper proposes a model predictive control based on the discrete Lyapunov function to improve the performance of power electronic converters. The proposed control technique, based on the finite control set model predictive control (FCS-MPC), defines a cost function for the control law which is determined under the Lyapunov stability theorem with a control error compensation. The steady state and dynamic performance of the proposed control strategy has been tested under a single phase AC/DC voltage source rectifier (S-VSR). Experimental results demonstrate that the proposed control strategy not only offers global stability and good robustness but also leads to a high quality sinusoidal current with a reasonably low total harmonic distortion (THD) and a fast dynamic response under linear loads.

Key words: Discrete Lyapunov function, Lyapunov stability theorem, Model predictive control, Power electronic converters, Robustness

I. INTRODUCTION

Power electronic converters provide many benefits to the economy and in people's livelihoods. The control strategies of converters have gradually become a research beacon in terms of the requirements of power quality [1]-[3].

With the development of high speed and powerful digital signal processors (DSPs) and microprocessors, growing attention and interest have been paid to the use of model predictive control (MPC) in power electronics. Generally, the MPC techniques applied to power electronics have been classified into two main categories: continuous control set MPC (CCS-MPC) and finite control set MPC (FCS-MPC) [4], [5]. In CCS-MPC, a modulator using sinusoidal pulse width modulation (SPWM) or space vector pulse width modulation (SVPWM) generates switching states starting from the continuous output of a predictive controller [6], [7]. On the other hand, FCS-MPC takes advantage of the discrete nature of power converters for solving optimization problems [8], [9]. Without the modulation stage, FCS-MPC applies direct control action to the converter.

The conventional FCS-MPC employs one voltage vector during one sampling period, and needs a high sampling frequency to achieve a better performance. In one sampling period, FCS-MPC consists of two main steps. The first step is prediction of the behavior for the next sampling instant for all possible voltage vectors and evaluation of the cost function for each prediction. The second step is to find the optimal voltage vector based on the traversal algorithm. This fact increases the computation burden [10]-[12]. Furthermore, due to the limited number of voltage vectors in the converter, the performance improvement caused by the conventional FCS-MPC is limited, and the THD of the controlled variable is higher than that of the conventional control based on a modulator [13], [14].

The Lyapunov function based control strategy is powerful for considering global stability and robustness. Several studies of this strategy have been published in the literature [15]-[21]. Using the discrete energy function to achieve

Manuscript received Nov. 16, 2016; accepted Mar. 27, 2017
Recommended for publication by Associate Editor Bon-Gwan Gu.
†Corresponding Author: gpdu@scut.edu.cn
Tel: +86-139-2646-0600, South China University of Technology
*School of Electric Power, South China University of Technology, China

superior performance and global asymptotic stability for the boost PFC converters in electric vehicles was presented in [15]-[17]. In [18]-[19], a Lyapunov function based control approach was applied for a single phase inverter with a LCL filter and a single phase inverter with a LC filter, respectively. In [20-21], a three phase AC-DC voltage source rectifier achieved a fast dynamic performance by adopting the Lyapunov function based control strategy. In particular, this control approach was modified with a model predictive control in [21]. In this paper, a model predictive control based on the discrete Lyapunov function is proposed to improve control performance by adding an error term of the controlled variable and the reference variable to the control law. The discrete model of the S-VSR and the principle of the conventional FCS-MPC are elaborately described in Section II. The control law is calculated using the Lyapunov stability theorem based on the discrete Lyapunov function and the proposed control strategy is given in Section III. In Section IV, the control coefficient, α, of the error term in the control law is selected by analyzing its influence on the steady state and the dynamic performance in terms of stability and robustness. In Section V, the performance of the proposed method for the S-VSR is investigated with an experimental system, and the experimental results are presented and compared with those obtained with the conventional FCS-MPC. Finally, some conclusions are drawn in Section VI.

II. CONVENTIONAL FCS-MPC

Fig. 1 shows an S-VSR. The equation describing the operation of the converter can be written as:

$$L_s \frac{di}{dt} = e - Ri - V_r \tag{1}$$

where:

e the grid voltage.
V_r the rectifier voltage.
i the grid current.
R the equivalent series resistance.
L_s the inductance of the line filter.

The discrete model of the converter is obtained to approximate the derivative di/dt in (1) by:

$$\frac{di}{dt} = \frac{i(k+1) - i(k)}{T} \tag{2}$$

where:

T the sampling time.

By substituting (2) into (1), the following expression is obtained for the future current at the (k+1)th instant. From (1), the equivalent eddy currents are straight-forwardly derived as follows:

$$i(k+1) = (1 - \frac{RT}{L_s})i(k) + \frac{T}{L_s}\left[e(k) - V_r(k+1)\right] \tag{3}$$

where:

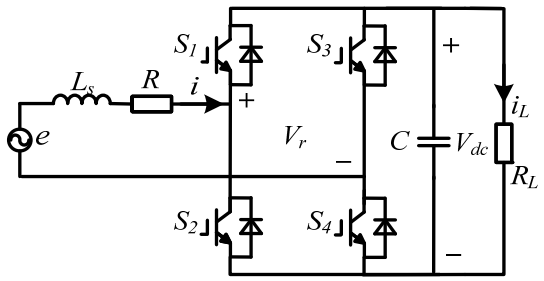

Fig. 1. Single phase AC/DC voltage source rectifier.

$V_r(k+1)$ is the future rectifier voltage of the S-VSR, and it is a continuous vector.

There are three voltage vectors that can predict three future current values. The conventional FCS-MPC method is based on this property.

$$i^p(k+1) = (1 - \frac{RT}{L_s})i(k) + \frac{T}{L_s}\left[e(k) - V(k+1)\right] \tag{4}$$

where:

$i^p(k+1)$ the future predicted current.

$V(k+1)$ the discrete voltage vector of the S-VSR, which is selected from the three voltage vectors 0, $-V_{dc}$ and V_{dc}.

Using this property, it is possible to use the following cost function to select the optimal switching state in the next step as:

$$J = \left| i^p(k+1) - i^*(k+1) \right| \tag{5}$$

where:

$i^*(k+1)$ the future reference current value.

The optimal future switching state selected from the cost function J can force the future current value to approach the reference current value in the next step. Finally, the selected voltage state, which can minimize the current error, is applied to the rectifier in the next sampling instant.

III. PROPOSED CONTROL STRATEGY BASED ON THE DISCRETE LYAPUNOV FUNCTION

An effective control algorithm is essential for the S-VSR so that the current, $i(k)$, tracks the reference value, $i^*(k)$. Therefore, it is necessary to find a control function where the current tracking error, $\Delta i(k)$, asymptotically converges to zero. The Lyapunov direct method is used for specific applications.

In addition, the error $\Delta i(k)$ is taken as:

$$\Delta i(k) = i(k) - i^*(k) \tag{6}$$

According to the Lyapunov stability theorem, the discrete Lyapunov function, $L(x(k))$, satisfies the following properties:

1) $L(0)=0$

2) $L(x(k))>0$ for all $x(k)\neq 0$

3) $L(x(k)) \rightarrow \infty$ as $\|x(k)\| \rightarrow \infty$

4) $\Delta L(x(k))<0$ for all $x(k)\neq 0$

Thus, the discrete Lyapunov function $L(\Delta i(k))$ of the S-VSR can be taken as:

$$L(\Delta i(k)) = \frac{1}{2}\Delta i^2(k) \tag{7}$$

From (6) and (7), the rate of change of the Lyapunov function, $L(\Delta i(k))$, can be expressed for the rectifier mode as:

$$\begin{aligned}\Delta L(\Delta i(k)) &= L(\Delta i(k+1)) - L(\Delta i(k)) \\ &= \frac{1}{2}\left[i(k+1) - i^*(k+1)\right]^2 \\ &\quad - \frac{1}{2}\left[i(k) - i^*(k)\right]^2\end{aligned} \tag{8}$$

To satisfy the Lyapunov stability theorem the following expression is defined as:

$$i(k+1) - i^*(k+1) = \alpha\left[i(k) - i^*(k)\right] \tag{9}$$

where α is a control coefficient with a constant value.

Substitute (9) into (8), and obtain the following expression for $\Delta L(\Delta i(k))$.

$$\begin{aligned}\Delta L(\Delta i(k)) &= L(\Delta i(k+1)) - L(\Delta i(k)) \\ &= \frac{1}{2}(\alpha^2 - 1)\left[i(k) - i^*(k)\right]^2\end{aligned} \tag{10}$$

It is apparent that $\Delta L(\Delta i(k)) < 0$, if α is chosen as:

$$0 < \alpha < 1 \tag{11}$$

The future control law $V_r(k+1)$ at the $(k+1)$th instant of the proposed control strategy can be determined with (3) and (9), and it can be written as:

$$\begin{aligned}V_r(k+1) &= e(k) + (\frac{L_s}{T} - R)i(k) - \frac{L_s}{T}i^*(k+1) \\ &\quad - \alpha\frac{L_s}{T}\left[i(k) - i^*(k)\right]\end{aligned} \tag{12}$$

It is clearly shown that (12) is related to the controlled variable $i(k)$ at the kth instant and the reference variable $i^*(k+1)$ at the $(k+1)$th instant. It is also related to the error term of the controlled variable and the reference variable at the kth instant. Therefore, the proposed control law has a feed forward and feedback structure which is the same as the model predictive control. In addition, when α=0, by solving (12), the control law can be expressed as:

$$\hat{V}_r(k+1) = e(k) + (\frac{L_s}{T} - R)i(k) - \frac{L_s}{T}i^*(k+1) \tag{13}$$

which is the same as the control law for the deadbeat control.

In the proposed strategy, the control law in (12) is used as the continuous future reference voltage vector to choose one of the three future voltage vectors of the S-VSR in a finite set. If the future voltage vector of the S-VSR closest to the future reference voltage vector obtained from (12) is applied to the S-VSR, the current at the next sampling instant can track the future reference current. Since the S-VSR only generates the three voltage vectors in their finite set in contrast to the continuous reference voltage vector in (12), the cost function defined as (14) allows one proper future voltage vector to be selected among the three possible vectors.

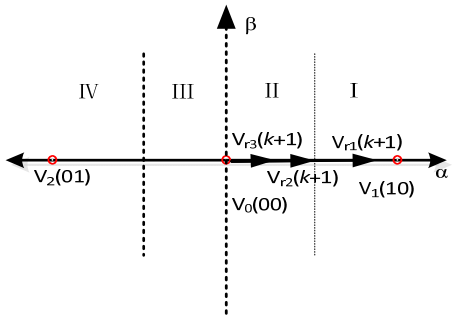

Fig. 2. Optimal voltage vector selection.

$$G = \left|V_r(k+1) - V(k+1)\right| \tag{14}$$

IV. Selection and Influence of the Control Coefficient

As shown in (12), the key point of the proposed control strategy is to increase the error term with the control coefficient, α, in the control law of the deadbeat control, and the selection of α is closely related to the control performance.

A. Influence of Stability

The discrete voltage vector applied to the rectifier in the next sampling period is regarded as the sum of the continuous future reference voltage vector and the quantization error vector is expressed as:

$$V(k+1) = V_r(k+1) + \Delta v(k+1) \tag{15}$$

Fig.2 shows the selection principle of the optimal voltage vector based on (15) in the positive period of $e(k)$. According to the cost function (14), the optimal voltage vector $V(k+1)$ minimizes G. From Fig.2 it can be seen that there are 3 cases for the future reference voltage vector $V_r(k+1)$ in the positive period of $e(k)$:

1): $V_r(k+1)$ is situated in Sector I as $V_{r1}(k+1)$. To minimize G, V_1 is selected. The quantization error vector satisfies $0 \le \Delta v(k+1) \le 0.5V_{dc}$.

2): $V_r(k+1)$ is situated in the juncture of Sector I and Sector II as $V_{r2}(k+1)$. To minimize G, V_1 or V_0 is selected. The quantization error vector satisfies $|\Delta v(k+1)| = 0.5V_{dc}$.

3): $V_r(k+1)$ is situated in Sector II as $V_{r3}(k+1)$. To minimize G, V_0 is selected. The quantization error vector satisfies $-0.5V_{dc} \le \Delta v(k+1) \le 0$.

The selection principle of the optimal voltage vector in the negative period of $e(k)$ is similar to that in positive period of $e(k)$. According to the analysis, the quantization error vector is bounded in:

$$\left\|\Delta v(k+1)\right\| \le 0.5V_{dc} \tag{16}$$

The direct Lyapunov method gives the following stability criteria for a function $L(\Delta i(k))$ and it is uniformly and ultimately bounded [22], i.e.:

$$\begin{aligned} &L(\Delta i(k)) \geq c_1 \left|\Delta i(k)\right|^l, \quad \forall \Delta i(k) \in G \\ &L(\Delta i(k)) \leq c_2 \left|\Delta i(k)\right|^l, \quad \forall \Delta i(k) \in \Gamma \\ &L(\Delta i(k+1)) - L(\Delta i(k)) < -c_3 \left|\Delta i(k)\right|^l + c_4 \end{aligned} \tag{17}$$

where c_1, c_2, c_3, and c_4 are positive constants, $l \geq 1$, $G \subseteq R_n$ is a positive control invariant set, and $\Gamma \subset G$ is a compact set.

By applying the value of the future voltage vector (15), $V(k+1)$, for the rectifier, the rate of change of the Lyapunov function, $\Delta L^p(\Delta i(k))$, can be written as:

$$\begin{aligned} \Delta L^p(\Delta i(k)) = &\frac{1}{2}[i^p(k+1) - i^*(k+1)]^2 \\ &-\frac{1}{2}[i(k) - i^*(k)]^2 \end{aligned} \tag{18}$$

By substituting (4) and (12) into (18), $\Delta L^p(\Delta i(k))$ can be written as:

$$\begin{aligned} \Delta L^p(\Delta i(k)) = &\frac{1}{2}(\alpha^2 - 1)\Delta i^2(k) \\ &+\frac{1}{2}\left[\frac{T}{L_s}\Delta v(k+1)\right]^2 \\ &-\alpha\frac{T}{L_s}\Delta v(k+1)\Delta i(k) \end{aligned} \tag{19}$$

Solving (19), it can be expressed as:

$$\begin{aligned} \Delta L^p(\Delta i(k)) = &(\frac{1}{2} - b)(\alpha^2 - 1)\Delta i^2(k) \\ &+ p(\Delta i(k)), \\ p(\Delta i(k)) = &\, b(\alpha^2 - 1)\Delta i^2(k) \\ &-\alpha\frac{T}{L_s}\Delta v(k+1)\Delta i(k) \\ &+\frac{1}{2}\left[\frac{T}{L_s}\Delta v(k+1)\right]^2 \end{aligned} \tag{20}$$

where b is a positive constant within $0<b<1/2$.

It is clear that $p(\Delta i(k))$ has a maximum, shown as (21), based on (11):

$$p(\Delta i(k))_{\max} = \left[\frac{T}{L_s}\Delta v(k+1)\right]^2 \frac{(1-2b)\alpha^2 + 2b}{4b(1-\alpha^2)} \tag{21}$$

As a result, by considering (16), the rate of the change of the Lyapunov function in (19) is:

$$\begin{aligned} &\Delta L^p(\Delta i(k)) \\ &\leq (\frac{1}{2} - b)(\alpha^2 - 1)\Delta i^2(k) + p(\Delta i(k))_{\max} \\ &\leq (\frac{1}{2} - b)(\alpha^2 - 1)\Delta i^2(k) \\ &\quad + \frac{1}{4}(\frac{T}{L_s}V_{dc})^2 \frac{(1-2b)\alpha^2 + 2b}{4b(1-\alpha^2)} \end{aligned} \tag{22}$$

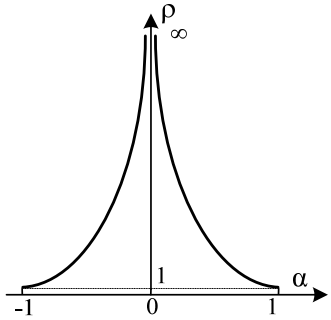

Fig. 3. The relationship between ρ and α.

Fig. 3 shows ρ as a function of α. It is clear that when α^2 is gradually increased from -1 to 1, ρ is decreased and the convergence speed is also decreased. It is well known that the convergence speed is closely related to dynamic performance.

Therefore, the stability condition (17) is satisfied by the constant values as:

$$\begin{aligned} &c_1 = c_2 = 1;\ c_3 = (\frac{1}{2} - b)(1 - \alpha^2); \\ &c_4 = \frac{1}{4}(\frac{T}{L_s}V_{dc})^2 \frac{(1-2b)\alpha^2 + 2b}{4b(1-\alpha^2)} \end{aligned} \tag{23}$$

In addition, (22) can be expressed as:

$$\Delta L^p(\Delta i(k)) \leq -2c_3 L^p(\Delta i(k)) + c_4 \tag{24}$$

This inequality implies that, as time increases, the current control error converges to the compact set as:

$$A = \left\{ \Delta i(k) \middle| \left\| \Delta i(k) \right\| \leq \sqrt{\frac{c_4}{c_3}} \right\} \tag{25}$$

It is clear that when α^2 is larger, the convergence domain is larger and the convergence domain is closely related to robustness.

B. Influence of Convergence Speed

From (8), the relationship between the Lyapunov function of the $(k+1)$th instant and the Lyapunov function of the kth instant can be described as:

$$L(\Delta i(k+1)) = \alpha^2 L(\Delta i(k)) \tag{26}$$

The convergence speed of the Lyapunov function can be studied using ρ, which is given by:

$$\rho = \frac{L(k)}{L(k+1)} = 1/\alpha^2 \tag{27}$$

C. Influence of Steady-State Performance

To study the effect of α on steady state performance, it is necessary to neglect the equivalent series resistance R and suppose that the current reference value does not change considerably in one sampling interval. The future current value can be expressed by:

$$i(k+1) = i(k) + \frac{T}{L_s}[e(k) - V_r(k+1)] \tag{28}$$

TABLE I
SYSTEM PARAMETERS

System parameters	Symbol	Value
AC voltage(RMS)	e	$50V/50Hz$
Filter inductance	L_s	$6mH$
Equivalent series resistance	R	0.3Ω
DC side capacitor	C	$1000\mu F$
DC side voltage	V_{dc}	$100V$
Sampling frequency	T	5e-5s

In addition, the continuous future reference voltage vector can be expressed by:

$$V_r(k+1) = e(k) + (1-\alpha)\frac{L_s}{T}\left[i(k) - i^*(k)\right] \tag{29}$$

In the positive period of $e(k)$, it is hoped that $i(k+1)$ is close to $i^*(k+1)$. When $i(k)>i^*(k)$ at the kth instant, the optimal voltage vector should be V_1. To increase the possibility of V_1 by increasing $V_r(k+1)$, the improved range of α is -1<α<0. When $i(k)<i^*(k)$ at the kth instant, the optimal voltage vector should be V_0. To increase the possibility of V_0 by decreasing $V_r(k+1)$, the improved range of α is also -1<α<0.

Therefore, the improved value range of α is given as:

$$-1 < \alpha < 0 \tag{30}$$

D. Selection of α

According to the above analyses, when α^2 is selected to be larger within the value range, the steady-state performance and robustness are improved. However, the convergence speed and dynamic performance are worse. Therefore, a compromise should be made during the selection of α. A typical range of α for the rectifier in this study is found to be:

$$-0.6 < \alpha < 0.2 \tag{31}$$

V. SIMULATION AND EXPERIMENTAL RESULTS

The proposed control strategy has been verified by simulation and experimental results. The simulations were carried out by MATLAB/Simulink. The experimental test was performed using a single phase PWM AC/DC voltage source rectifier prototype in a DSP system based on a TMS320F28069. The system parameters are given in Table I.

Fig.4 shows simulation results of the steady-state error of $i(k)$ based on different values of α. It is clear that the smaller the value of α, the better the steady-state performance. In this paper, α is selected as −0.45 in the experimental test.

A. Simulation Results

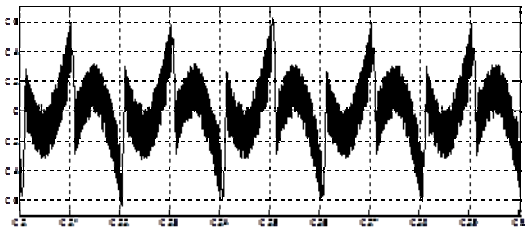

(a) α=0.2.

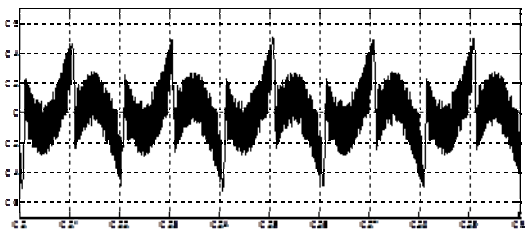

(b) α=0.

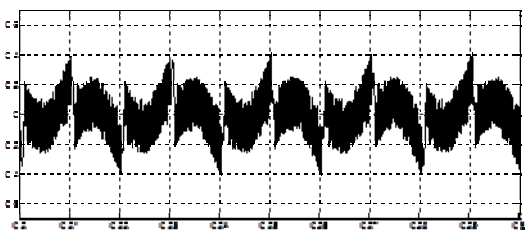

(c) α=−0.2.

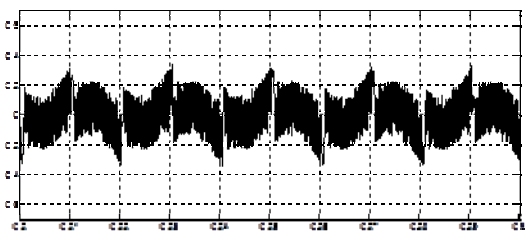

(d) α=−0.5.

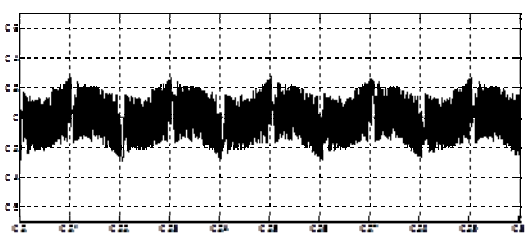

(e) α=−0.8.

Fig. 4. Simulated error $\Delta i(k)$ in the steady state based on different values of α (0.2A/div).

B. Steady-state Response Tests

Fig. 5 shows the steady-state test results of the proposed control strategy when the reference current peaks at 6.8 A. Fig.5(a) depicts the input current and voltage waveforms, where current follows the voltage to achieve a unit power factor. Fig.5(b) is the harmonic spectrum of the current. These test results demonstrate the improved steady-state response of the proposed control strategy. The converter

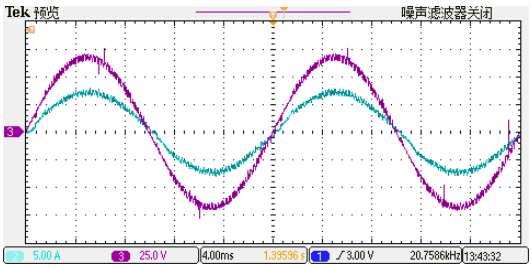

(a) Voltage and current waveforms.

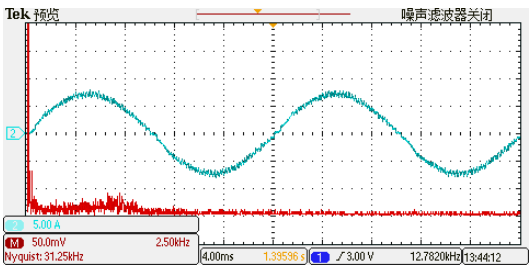

(b) Harmonic spectrum of the current.

Fig. 5. Steady-state test results of the proposed control strategy (α=−0.45).

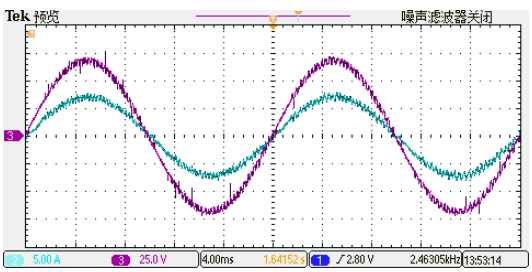

(a) Voltage and current waveforms.

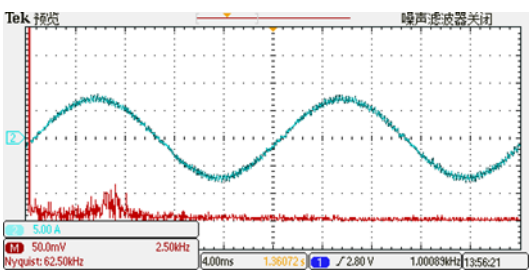

(b) Harmonic spectrum of the current.

Fig. 6. Steady state test results of the conventional FCS-MPC.

input current is highly sinusoidal with a measured total harmonic distortion (THD) of 2.16%.

Fig. 6 shows test results of the conventional FCS-MPC. As observed from the current waveforms, the fluctuation range of the current is larger, and the THD is 3.38%.

Fig.7 shows test result of the online parameter estimation control method referred in [23]. The THD of the current waveform is 2.51%. From the comparison above, it can be seen that the proposed control method has the best steady-state response, followed by the online parameter estimation FCS-MPC control method. The steady-state test results of the conventional FCS-MPC are the worst.

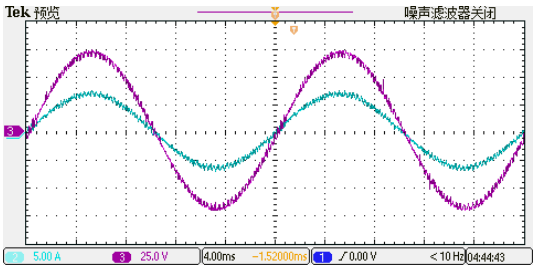

(a) Voltage and current waveforms.

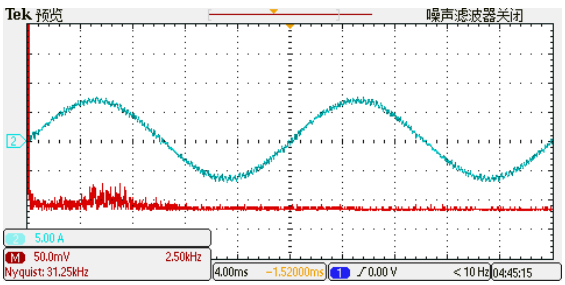

(b) Harmonic spectrum of the current.

Fig. 7. Steady-state test results of the online parameter estimation control strategy in [23].

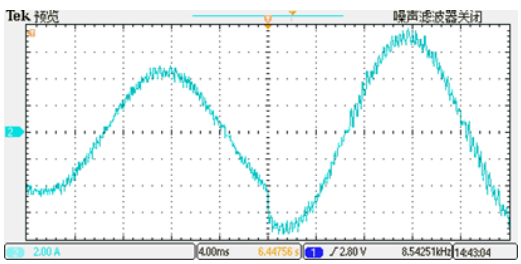

(a) Step change from 4- to 6.8- A peak.

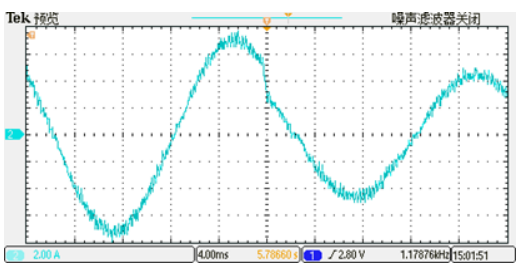

(b) Step change from 6.8- to 4- A peak.

Fig. 8. Current behavior during a reference step with the proposed control strategy (α=−0.45).

C. Dynamic Response Tests

An important aspect of any control system is the dynamic response to changes in the reference. Fig.8 depicts the current behavior with the proposed control strategy (α=−0.45) when the reference step changes from 4- to 6.8- A peak and vice versa. The current reached a steady-state level in Fig.8(a) within 126μs and requires 268μs to reach a steady state in Fig. 8(b). Compared with the proposed control strategy, the conventional FCS-MPC has a faster dynamic response as shown in the analysis in section IV. Fig.9 shows the

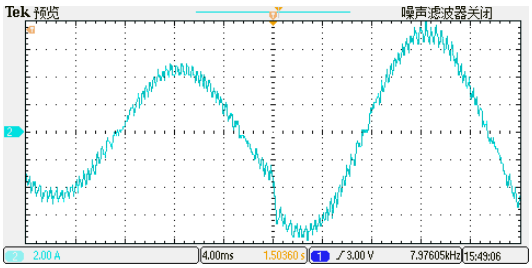

(a) Step change from 4- to 6.8- A peak.

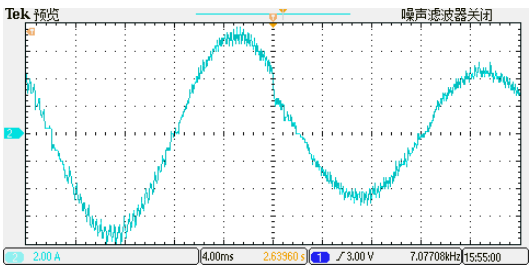

(b) Step change from 6.8- to 4- A peak.

Fig. 9. Current behavior during a reference step with the conventional FCS-MPC.

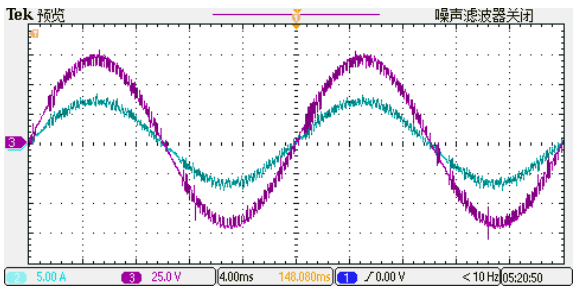

(a) *L* mismatch with -25%.

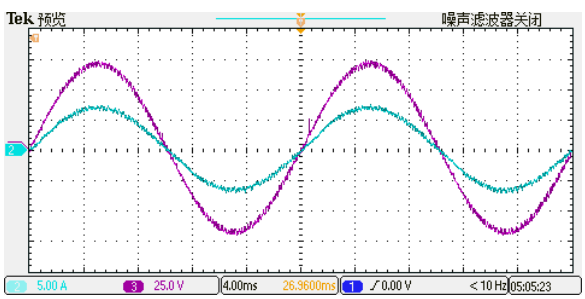

(b) *L* mismatch with +25%.

Fig. 10. Steady-state test result of the proposed control strategy when the inductance *L* has a mismatch.

current behavior with the conventional FCS-MPC when the reference step changes from 4- to 6.8- A peak and from 6.8- to 4- A peak. The dynamic response time in Fig. 9(a) is 107μs and that in Fig.9(b) is 231μs. These experiment results are consistent with the analysis in Section IV.

D. Robustness Tests

System parameters, such as the inductance and equivalent resistance, vary with temperature, core saturation, and other environmental conditions. In addition, parameter errors influence the whole control performance. The robustness of the proposed control strategy is tested when the actual inductance is mismatched by -25% and +25%.

Fig. 10 shows steady-state test results of the proposed control strategy when the inductance has a mismatch of -25% and +25%. It can be seen that when the inductance has a mismatch of -25%, there are higher input current ripples. However, inductance mismatch does not influence the system stability in the proposed control strategy.

VI. Conclusions

A model predictive control based on the discrete Lyapunov function with control error compensation of power electronic converters is proposed in this paper. The criterion for selecting the control coefficient, α, is described. Furthermore, the influence of changing α is also studied.

The proposed control strategy, based on the discrete direct Lyapunov method, leads to a globally asymptotically stable system. In addition, it shows improved steady-state performance and has a fast dynamic response that is just a little slower than the conventional FCS-MPC. The results associated in this investigation are very encouraging and will continue to play a strategic role in the improvement of modern digital control systems.

References

[1] M. P. Kazmierkowski, R. Krishnan, and F. Blaabjerg, *Control in Power Electronics*, New York, NY, USA: Academic, 2002.

[2] J. R. Rodriguez, J. W. Dixon, J. R. Espinoza, J. Pontt, and P. Lezana, "PWM regenerative rectifiers: State of the art," *IEEE Trans. Ind. Electron*., Vol. 52, No. 1, pp. 5–22, Feb. 2005.

[3] F. Blaabjerg, R. Teodorescu, M. Liserre, and A. V. Timbus, "Overview of control and grid synchronization for distributed power generation systems," *IEEE Trans. Ind. Electron*., Vol. 53, No. 5, pp. 1398–1409, Oct. 2006.

[4] P. Cortes, M. P. Kazmierkowski, R. M. Kennel, D. E. Quevedo, and J. Rodriguez, "Predictive control in power electronics and drives," *IEEE Trans. Ind. Electron*., Vol. 55, No. 12, pp. 4312–4324, Dec. 2008.

[5] S. Vazquez, J. I. Leon, L. G. Franquelo, J. Rodriguez, H. A. Young, A. Marquez, and P. Zanchetta, "Model predictive control: A review of its applications in power electronics," *IEEE Ind. Electron. Mag.*, Vol. 8, No. 1, pp. 16–31, Mar. 2014.

[6] M. Preindl and E. Schaltz, "Sensorless model predictive direct current control using novel second order PLL-observer for PMSM drive systems," *IEEE Trans. Ind. Electron.*, Vol. 58, No. 9, pp. 4087-4095, Sep. 2011.

[7] S. Mariethoz, A. G. Beccuti, G. Papafortiou, and M. Morari, "Sensorless explicit model predictive control of the DC-DC buck converter with inductor current limitation," in *Twenty-Third Annual IEEE Applied Power Electronics Conference and Exposition (APEC)*, pp. 1710-1715, Feb. 2008.

[8] J. Rodriguez, J. Pontt, C. A. Silva, P. Correa, P. Lezana, P.

Cortes, and U. Ammann, "Predictive current control of a voltage source inverter," *IEEE Trans. Ind. Electron.*, Vol. 54, No. 1, pp. 495-503, Feb. 2007.
[9] M. A. Perez, P. Cortes, and J. Rodriguez, "Predictive control algorithm technique for multilevel asymmetric cascaded H-bridge inverters," *IEEE Trans. Ind. Electron.*, Vol. 55, No. 12, pp. 4354-4361, Dec.2008.
[10] P. Cortes, J. Rodriguez, C. Silva, and A. Flores, "Delay compensation in model predictive current control of a three-phase inverter," *IEEE Trans. Ind. Electron*., Vol. 59, No. 2, pp. 1323–1325, Feb. 2012.
[11] Y. Zhang, W. Xie, Z. Li, and Y. Zhang, "Low complexity model predictive power control double vector-based approach," *IEEE Trans. Ind. Electron.*, Vol. 61, No. 11, pp. 5871-5880, Nov. 2014.
[12] C. Xia, T. Liu, T. Shi, and Z. Song, "A simplified finite control set model predictive control for power converters," *IEEE Trans. Ind. Informat.*, Vol. 10, No. 2, May 2014.
[13] H. A. Young, M. A. Perez, J. Rodriguez, H. Abu-Rub, "Assessing finite-control-set model predictive control: a comparison with a linear current controller in two-level voltage source inverters," *IEEE Ind. Electron. Mag.*, Vol. 8, No. 1, pp. 44-52, Mar. 2014.
[14] R. P. Aguilera, P. Lezana, and D. E. Quevedo, "Switched model predictive control for improved transient and steady-state performance," *IEEE Trans. Ind. Informat.*, Vol. 11, No. 4, pp. 968-977, Aug. 2015.
[15] P. Das, M. Pahlevaninezhad, J. Drobnik, G. Moschopoulos, and P. K. Jain, "Nonlinear controller based on a discrete energy function for an AC/DC boost PFC converter," *IEEE Trans. Power Electron.,* Vol. 28, No. 12, pp. 5458-5476, Dec. 2013.
[16] M. Pahlevaninezhad, P. Das, J. Drobnik, P. K. Jain, and A. Bakhshai, "A new control approach based on the differential flatness theory for an AC/DC converter used in electric vehicles," *IEEE Trans. Power Electron.*, Vol. 27, No. 4, pp. 2085-2103, Apr. 2012.
[17] M. Pahlevaninezhad, P. Das, J. Drobnik, G. Moschopoulos, P. K. Jain, and A. Bakhshai, "A nonlinear optimal control approach based on the control-Lyapunov function for an AC/DC converter used in electric vehicles," *IEEE Trans. Ind. Informat.*, Vol. 8, No. 3, pp. 596-614, Aug. 2012.
[18] H. Komurcugil, N. Altin, S. Ozdemir, and I. Sefa, "Lyapunov-function and proportional-resonant based control strategy for single-phase grid connected VSI with LCL filter," *IEEE Trans. Ind. Electron*., Vol. 63, No. 5, pp. 2838–2849, May 2016.
[19] H. Komurcugil, N. Altin, S. Ozdemir, and I. Sefa, "An extended Lyapunov-function-based control strategy for single-phase UPS inverters," *IEEE Trans. Power Electron.*, Vol. 30, No. 7, pp. 3976–3983, Jul. 2015.
[20] H. Komurcugil and O. Kukrer, "Lyapunov-based control for three-phase PWM AC/DC voltage-source converters," *IEEE Trans. Power Electron*., Vol. 13, No. 5, pp. 801–813, Sep. 1998.
[21] M. P. Akter, S. Mekhilef, N. M. L. Tan, and H. Akagi, "Modified model predictive control of a bidirectional AC-DC converter based on Lyapunov function for energy storage systems," *IEEE Trans. Ind. Electron.*, Vol. 63, No. 2, pp. 704–715, Feb. 2016.
[22] J.-J. E. Slotineand and W. Li, *Applied Nonlinear Control*, Englewood Cliffs, NJ, USA: Prentice-Hall, 1991.
[23] S.-J. Jeong and S.-H. Song, "Improvement of predictive current control performance using online parameter estimation in phase controlled rectifier," *IEEE Trans. Power Electron*., Vol. 22, No. 5. pp. 1820-1825, Sep. 2007.

Guiping Du was born in Gansu province, China, in 1968. He received his B.S. and M.S. degrees in Electrical Engineering from Southwest Jiaotong University, Chengdu, China, in 1990 and 1997, respectively; and his Ph.D. degree from the South China University of Technology, Guangzhou, China, in 2003. He is presently working as a Professor in the Department of Electric Power, South China University of Technology. His current research interests include power electronic systems and digital control, including wireless power transmission, high power high frequency industrial power supply devices, motor monitoring, energy-saving management systems, and model predictive control.

Zhifei Liu was born in Henan province, China, in 1986. He received his B.S. degree in Electrical Engineering from East China Jiaotong University, Nanchang, China, in 2009. He is presently working towards his M.S. degree in Power Electronics and Electrical Drives at the South China University of Technology, Guangzhou, China. His current research interests include power electronics and control, including AC/DC rectifiers and model predictive control.

Fada Du was born in Hubei province, China, in 1992. He received his B.S. degree in Electrical Engineering from the Beijing Institute of Technology, Beijing, China, in 2015. He is presently working towards his M.S. degree in Power Electronics and Electrical Drives at the South China University of Technology, Guangzhou, China. His current research interests include power electronics and control, including VIENNA AC/DC rectifiers and model predictive control.

Jiajian Li was born in Guangdong province, China, in 1992. He received his B.S. degree in Electrical Engineering from the South China University of Technology, Guangzhou, China, in 2016. He is presently working towards his M.S. degree in Power Electronics and Electrical Drives at the South China University of Technology, Guangzhou, China. His current research interests include power electronics and control, including DC/AC inverters and model predictive control.